PROCEEDINGS OF SPIE

SPIEDigitalLibrary.org/conference-proceedings-of-spie

Euclid imaging channels: from science to system requirements

J. Amiaux, J. L. Augueres, O. Boulade, C. Cara, S. Paulin-Henriksson, et al.

J. Amiaux, J. L. Augueres, O. Boulade, C. Cara, S. Paulin-Henriksson, A. Réfrégier, S. Ronayette, A. Amara, A. Glauser, C. Dumesnil, A. M. Di Giorgio, J. Booth, M. Schweitzer, R. Holmes, M. Cropper, E. Atad-Ettedgui, L. Duvet, D. Lumb, "Euclid imaging channels: from science to system requirements," Proc. SPIE 7731, Space Telescopes and Instrumentation 2010: Optical, Infrared, and Millimeter Wave, 77311I (5 August 2010); doi: 10.1117/12.857030

Event: SPIE Astronomical Telescopes + Instrumentation, 2010, San Diego, California, United States

Euclid Imaging Channels: from science to system requirements

J. Amiaux*[a], J.L. Augueres [a], O. Boulade [a], C. Cara [a], S. Paulin-Henriksson [a], A. Réfrégier [a], S. Ronayette [a], A. Amara [b], A. Glauser [b, c], C. Dumesnil [d], A.M. Di Giorgio [e], J. Booth [f], M. Schweitzer [g], R. Holmes [h], M. Cropper [i], E. Atad-Ettedgui [c], L. Duvet [j], D. Lumb [j]

[a]Service d'Astrophysique, Commissariat à l'Énergie Atomique, Orme des Merisiers, Bat 709, 91191 Gif sur Yvette, France;
[b]ETH Hoenggerberg Campus, Physics Department, HIT J 12.2, CH-8093 Zurich, Switzerland;
[c]UK Astronomy Technology Centre, Royal Observatory, Blackford Hill, Edinburgh EH9 3HJ, UK;
[d]Institut d'Astrophysique Spatiale, CNRS/Université Paris Sud 11, Orsay, France ;
[e]Istituto Fisica dello Spazio Interplanetario, INAF, Via Fosso del Cavaliere 100, 00143 Roma, Italy;
[f]Jet Propulsion Laboratory, 4800 Oak Grove Drive, MS 233-200, Pasadena, CA 91109, USA
[g]Max-Planck-Institut für Extraterrestrische Physik, 85748, Garching, Germany
[h]Max-Planck-Institut für Astronomie, Königstuhl 17, 69117, Heidelberg, Germany
[i]Mullard Space Science Laboratory, University College London, Holmbury St Mary, Dorking Surrey RH5 6NT, United Kingdom
[j]Science and Robotic Exploration1, Technical and Quality Management2, European Space Agency, ESTEC, Postbus 299, 2200AG Noordwijk, The Netherlands

ABSTRACT

Euclid is an ESA Cosmic Vision wide-field space mission concept dedicated to the high-precision study of Dark Energy and Dark Matter. The mission relies on two primary cosmological probes: Weak gravitational Lensing (WL) and Baryon Acoustic Oscillations (BAO).

The first probe requires the measurement of the shape and photometric redshifts of distant galaxies. The second probe is based on the 3-dimensional distribution of galaxies through spectroscopic redshifts. Additional cosmological probes are also used and include cluster counts, redshift space distortions, the integrated Sachs-Wolfe effect (ISW) and galaxy clustering, which can all be derived from a combination of imaging and spectroscopy.

Euclid Imaging Channels Instrument of the *Euclid* mission is designed to study the weak gravitational lensing cosmological probe. The combined Visible and Near InfraRed imaging channels form the basis of the weak lensing measurements. The VIS channel provides high-precision galaxy shape measurements for the measurement of weak lensing shear. The NIP channel provides the deep NIR multi-band photometry necessary to derive the photometric redshifts and thus a distance estimate for the lensed galaxies.

This paper describes the Imaging Channels design driver requirements to reach the challenging science goals and the design that has been studied during the Cosmic Vision Assessment Phase.

Keywords: *Euclid*, Dark Energy, Weak Lensing, System Architecture

1. INTRODUCTION

Euclid is one of the 3 remaining candidates of ESA cosmic vision program, among which 2 missions will be selected next year for a launch scheduled in 2017/2018. The primary goal of this mission is to map the geometry and evolution of the dark universe with unprecedented precision in order to place high accuracy constraints on Dark Energy, Dark Matter, Gravity and cosmic initial conditions[1]. This mission will use two independent cosmological probes: weak gravitational lensing (WL) and baryonic acoustic oscillations (BAO).

Space Telescopes and Instrumentation 2010: Optical, Infrared, and Millimeter Wave,
edited by Jacobus M. Oschmann Jr., Mark C. Clampin, Howard A. MacEwen, Proc. of SPIE
Vol. 7731, 77311I · © 2010 SPIE · CCC code: 0277-786X/10/$18 · doi: 10.1117/12.857030

For this purpose, *Euclid* will measure the shape and spectra of galaxies over the entire extragalactic sky in the visible and Near Infrared, out to redshift 2, thus covering the period over which dark energy accelerated the universe expansion (<10 Billion years).
The payload baseline comprises wide field instruments (0.5 deg2): an imaging instrument comprising a visible and a NIR channel, and a NIR spectroscopic instrument. The visible channel is used to measure the shapes of galaxies for weak lensing, with a resolution of 0.18 arcsec in a wide visible red band (R+I+Z, 0.55 to 0.92 µm). The NIR photometric channel provides three NIR bands (Y, J, H, spanning 1.0 to 2.0 µm) with a resolution of 0.300 arcsec.
The baseline for the NIR spectroscopic channel operates in the wavelength range 1.0 to 2.0 µm in slitless mode at a spectral resolution R=500, employing 0.500 arcsec pixels.

With this capability, the *Euclid* imaging instrument will contribute to the four *Euclid* primary science objectives in fundamental cosmology: (1) *Euclid* will measure the dark energy equation of state parameters w_0 and w_a to a precision of 2% and 10% from the geometry and structure growth of the Universe. *Euclid* will thus achieve a Dark Energy Figure of Merit of 500 (1500) without (with) Planck Priors, thus improving by a factor of 50 (150) upon current knowledge. (2) *Euclid* will test the validity of General Relativity against modified gravity theories, and measure the growth factor exponent to an accuracy of 2%. (3) *Euclid* will study the properties of dark matter by mapping its distribution, testing the Cold Dark Matter paradigm and measuring the sum of the neutrino masses to a few 0.01 eV in combination with Planck. (4) *Euclid* will improve the constraints on the initial condition parameters by a factor of 2-30 compared to Planck alone.

2. WEAK LENSING SURVEY KEY PARAMETERS

Probing dark energy and dark matter through weak lensing measurements requires to study the galaxy shapes spatial correlation induced by gravitational lensing. Deflection of light by the integrated mass distribution along the observer line of sight causes slight modifications of the distant galaxies image shapes. This effect is clearly visible in the case of strong gravitational lensing, when the mass density in a lens is above a critical threshold, the appearance of the background object is highly distorted with a characteristic pattern (see figure 1).

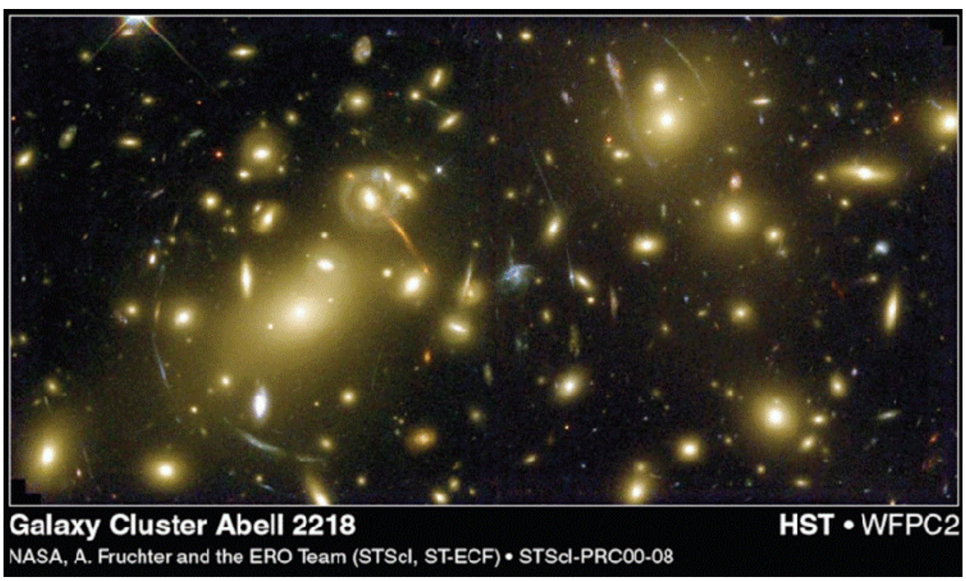

Figure 1. Illustration of strong gravitational lensing effects (Abell Cluster 2218 - W. Couch et al., 1975 – HST).

In the weak lensing regime that we are probing on large scale structures, the shear induced by gravitational effects on the large majority of objects is very faint. Typical variation of the original object ellipticity is of the order of magnitude of 1% and need to be measured with even higher accuracy (error 0.01%).

In order to measure shape parameters with accuracy on galaxies of typical size 0.3 to 0.4 arcsec, the galaxies are best observed in visible, that ensure accurate resolution (for a given telescope resolution scales as λ) and high sensitivity at peak emission of galaxy (bulge+disk). A single visible waveband is used on Euclid, extended toward the red-end of visible spectrum (R+I+Z, 550-920 nm) in order to match galaxy spectrum of redshifted galaxies. As most of the galaxies observed will be small, the shape measurement is achievable with adequate sampling using a 0.100 arcsec visible pixel platescale.

The data processing that allows measurement of the shape parameters, and especially the ellipticity of the galaxy, with the accuracy required for weak lensing is challenging and not defined yet. But whatever the method, it will require exquisite a priori knowledge of the image degradation process introduced by the instrument in order to correct the final image blurred by the Point Spread Function of the imaging system (optics, satellite jitter, detector), with various noise contributions and detector Charge Transfer Inefficiency trailing effects (see figure 2 for illustration of those effects on a galaxy).

To recover the shear information, the Point Spread Function is needed at galaxy location but will be measured on stars available from the observed field. Since instrument PSF varies on spatial scales of the field of view, and with time, it is necessary to calibrate the PSF model with stars surrounding the studied galaxies. Star images are pixelised and noisy, and their sampling is worse than for the galaxies (typical system PSF size is 0.200 arcsec). The content of information required for PSF calibration and interpolation can only be obtained by combining the information from several PSF (typically 50 stars). This fixes the constraints on the intrinsic ellipticity of the system PSF (ellitpicity in terms of weighted quadrupoles shall be < 10%) and on its stability on small field scales (stability over 50 arcmin² shall be better than $2.0x10^{-4}$).

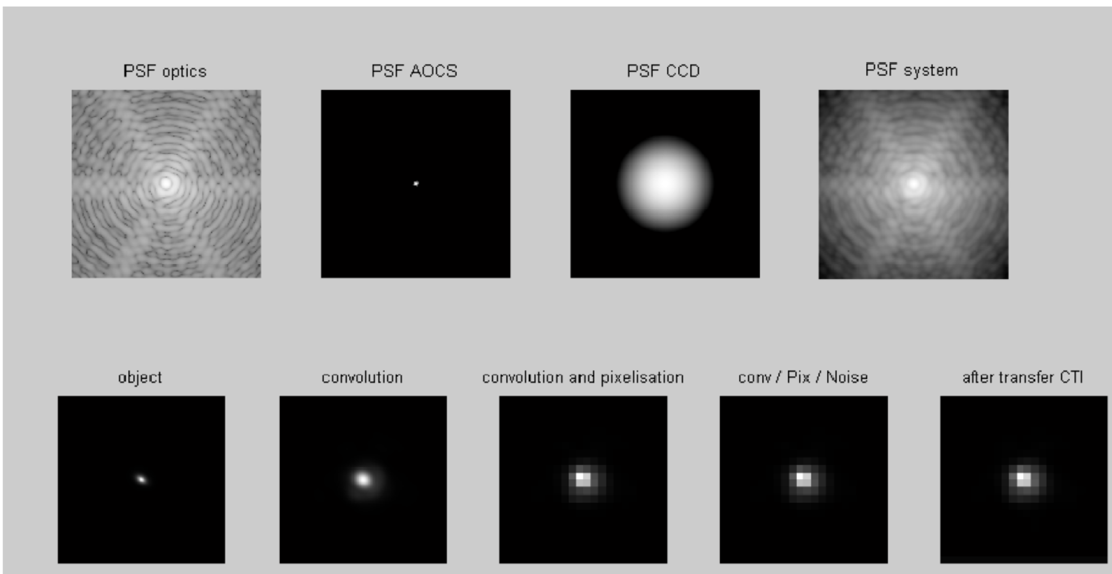

Figure 2. Illustration of the image degradation process, the object (galaxy) is convolved by the system PSF of the instrument (Optics, Attitude and Orbit Control System jitter, CCD), additive noise comes from various contributors (source, background, detection chain) and the CCD functioning mode introduces further signal shape modifications by trapping electrons during the read out.

Even with the extreme accuracy of shape measurement, the observer never has access to the initial shape of the object and therefore the shear information of a single object is not observable. The cosmic shear mapping on large scales can only be accessed on statistical basis, the underlying assumption being that intrinsic galaxy shapes are uncorrelated and therefore on average the mean ellipticity of a sample of galaxies in the absence of cosmic shear is zero.

The current weak lensing surveys (limited to a few 10's deg²) still have their uncertainties driven by the statistical errors (cosmic variance) linked to their limited sky coverage. In order to reach the accuracy claimed by Euclid mission, the survey must extend to the point where the number of galaxies allows overcoming the statistical uncertainties (typically over 2 billion galaxies). It has been assessed within the Euclid consortium that the most efficient approach to improve statistical accuracy is to enlarge the size of the survey rather than its depth (see figure 3).

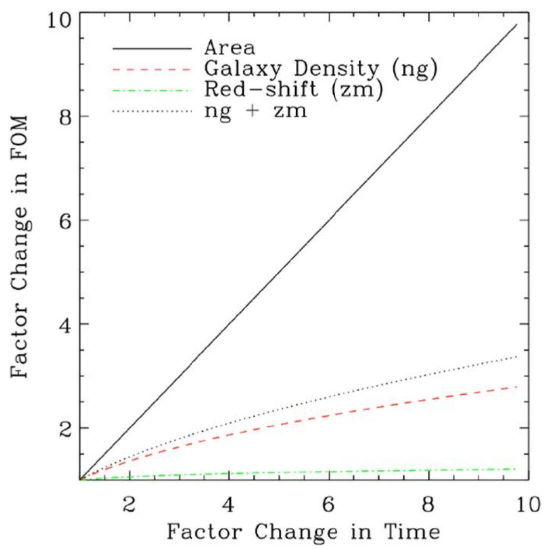

Figure 3. Gain in survey figure of merit with shear tomography when increasing survey time is allocated to area, galaxy density or median redshift (area vs. depth trade off) (from Amara & Réfrégier 2007 [3])

Studies for optimal survey performed within the Euclid Consortium[3] show that the typical 2 billion galaxies required for accurate cosmic shear measurement (1% precision on w) are better observed with an all extra-galactic sky survey of 20 000 deg² and shallow depth (z~0.8 to 1) with galaxy density between 30 and 40 galaxies per arcmin² than with deeper and smaller surveys.

The reference sky covered by Euclid survey will therefore be the whole extra galactic sky representing a 20 000 deg² area. This survey is illustrated in figure 4, showing the variation of detected galaxy density on the sky with zodiacal background (loss of area due to bright stars and extinction not shown on this figure) with instrument relevant scales of instrument and detectors Field of View.

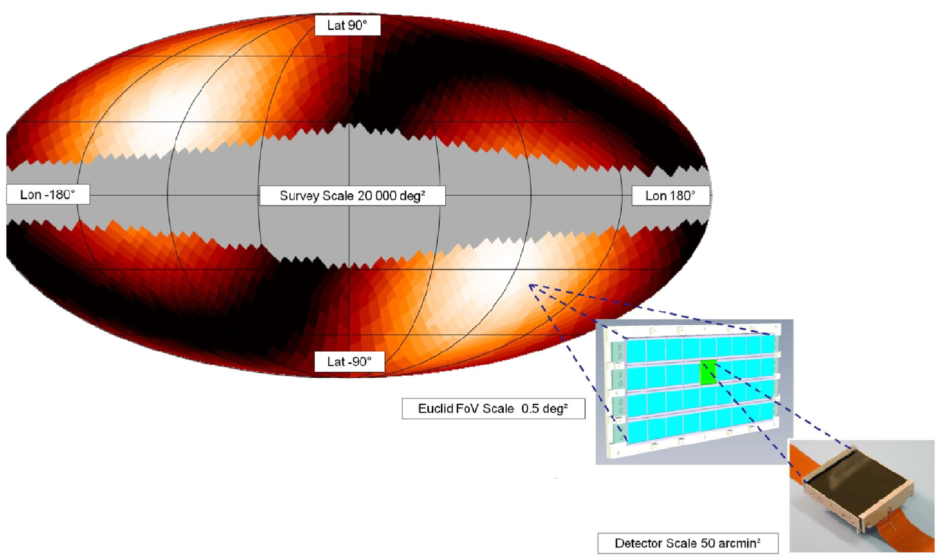

Figure 4. *Euclid* Survey and associated instrument relevant scales (instrument and detector typical field of view)

Weak lensing imaging only gives access to a 2-dimensional information on the shape of objects. But gravitational lensing is a 3-dimensional process integrating the deflection of light by the mass distribution all along the line of sight between the observer and the distant galaxy. It is assessed today that without redshift information for the lensed sources, weak lensing cannot provide reliable information on cosmological parameters. Adding a distance (or redshift) information in order to perform weak lensing tomography helps disentangling the line of sight projection effect and increase the understanding of structure.

Spectroscopically measuring the redshifts of the galaxies over the entire area of Euclid lensing survey is not feasible. Therefore, an alternative approach has been developed and tested in recent years: photometric redshifts. Individual galaxies are observed in different broad band filters and binned into a number of redshift bins (typically 10 bins).

Photo-z simulation in order to optimize the observation and binning strategy are performed in two groups within the Euclid consortium (see Abdalla[5] et al, and Bordoloi et al[6]) leading to the selection of a three Near Infrared wavebands strategy in the Y [920-1146 nm], J [1146-1371 nm] and extended H [1371-2000 nm] bands. The final photo-z accuracy will be achieved using these 3 NIR bands in addition of the visible band and complemented by ground based photometry (combination of DES and Pan-STARRS2 at minimum).

The redshift information is required at two conceptually distinct steps. First, each galaxy must be assigned to individual redshift bins. The shear signal is then extracted from the cross-correlation of the shape measurements of individual galaxies in different redshift bins, to exclude potential problems such as intrinsic alignments between physically associated galaxies that could be mistaken with coherent alignment produced by weak lensing. The required accuracy on individual photo-z for bin construction is set by the need to minimize overlap between the bins and hence remove physically close correlated galaxy pairs (Bridle and King[4]). The dispersion σz on NIR individual Photo-z is required to be less than 0.05(1+z) Once the weak lensing signal is extracted, a systematic precision in the mean z in each bin is set by the required accuracy of the cosmological parameters (Bordoloi et al, 2009[6]) and shall be $\sigma_{<z>} < 0.002(1+z)$.

In order to reach the photometric accuracy associated to photo-z requirements, the NIR plate scale needs to be 0.300 arcsec.

As the number of galaxies available in both visible and NIR is the key parameter to the statistical accuracy of the survey, image simulations of the sky as-seen by Euclid have been performed by 2 teams within the Euclid Consortium (see Meneghetti et al[7] and Massey et al[8], figure 5) in order to assess the depth of the survey needed to reach the required galaxy density and total number of objects available (~2 billion galaxies required). Image simulations show that with magnitude AB = 24.5 (10-σ) in the VIS and magnitude AB = 24.0 in the NIR (5-σ) a density between 30 and 40 galaxies per arcmin² are reached with Euclid observation sequence assumption, leading to ~2.5 10^9 galaxies available.

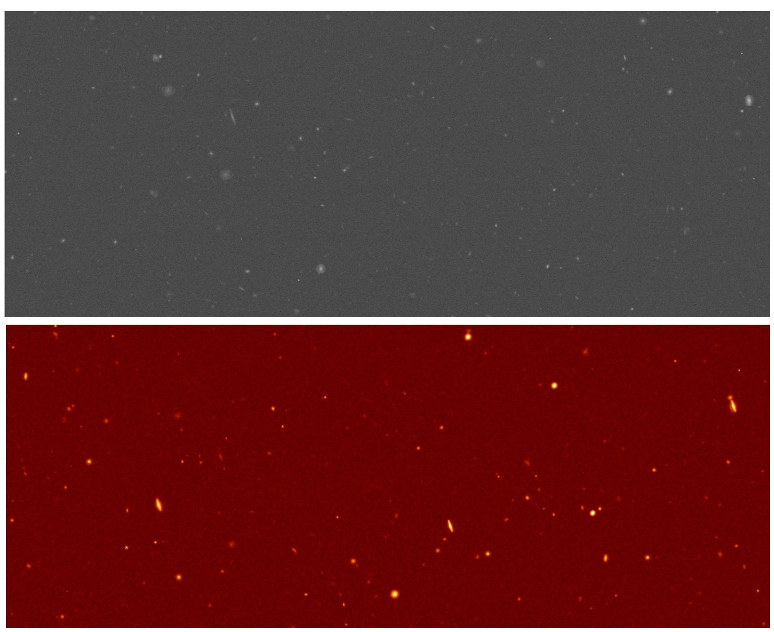

Figure 5. *Euclid* Visible R+I+Z band (top) and NIR J band (bottom) image simulations (courtesy M. Meneghetti).

Euclid Weak Lensing Tomography survey as described in this section and with the key parameters summarized in table 1, is designed to perform unprecedented accuracy cosmology measurements by minimizing the statistical source of errors.

N#	Key Parameter Definition
1	Shear effect ~1% of object ellipticity measured with error +/-0.01%
2	Shape measurement shall be performed in a single visible waveband R+I+Z, 550-920 nm
3	The sampling of galaxy for shape measurement shall be 0.100 arcsec
4	System PSF ellitpicity (in terms of weighted quadrupoles) shall be < 10% and stability over 50 arcmin^2 shall be better than 2.0 10-4.
5	N# galaxies > 2.109
6	Survey size 20 000 deg^2
7	weak lensing survey depth z~0.8 to 1
8	Photo-z measure in Y [920-1146 nm], J [1146-1371 nm] and extended H [1371-2000 nm] bands
9	NIR individual Photo-z dispersion $\sigma z<0.05(1+z)$
10	NIR Photo-z systematic precision in the mean z in each bin shall be $\sigma<z><0.002(1+z)$
11	Depth in R+I+Z: mAB=24.5 at 10-sigma (on extended source 0.3 arcsec diametre)
12	Depth in NIR YJH: mAB=24.0 at 5-sigma (on point source)
13	The plate scale in the NIR channel shall be 0.300 arcsec

Table 1. *Euclid* Survey key parameters summary

The key issue is now to control the level of systematic errors to confine them to a level where their contribution to the error on the dark energy equation of state parameters is minor compared to statistical errors.

Main systematic error source can be identified as follow:

- Interpretation of the shear signal (dark matter non-linear correction function, intrinsic alignment correction)
- Instrumental effects leading to ellipticity correlation (optical PSF anisotropy linked to distortion or diffraction pattern, detector effects, satellite line of sight jitter)
- Photometric redshift calibration errors.

Part of those systematic effects is linked to the improvement of science understanding and data processing. Some of them related to instrument calibration are directly impacting the mission and instrument design and definition described in section 3.

3. EUCLID IMAGING CHANNELS ARCHITECTURE

3.1 Mission definition

Observing a homogeneous survey of the entire extragalactic sky with minimum and controlled source of systematic effects, together with the request for shape measurement of high and stable image quality, and for photo-z observation in the IR that are filtered by the earth atmosphere, drive the Euclid survey to be a space mission.

Space observations provide diffraction limited imaging capabilities (no atmosphere turbulence perturbation) and optimal detection capabilities (no atmospheric attenuation) but of course at a price on instrument size and mass limitation, and increased cost and complexity of the overall program.

Following orbit evaluations performed during the Euclid Assessment Phase by ESA, the selected baseline is a large amplitude free-insertion libration orbit around the Sun-Earth second Lagrange point (SEL2 or L2).

The main advantage of this orbit is that Euclid wide survey can be performed in a very stable thermal environment which is preferred to limit the instrument PSF variations with time, and within a radiation environment less severe than Earth, which is the limiting factor for detector life time and degradations. Being at L2, such as for JWST or Herschel missions, introduces a constraint on the maximum telemetry rate achievable in K-band which sets the maximum to 850 Gbits of data that can be down-linked on a daily basis. The second limitation is coming from the Soyouz launcher selected, that sets the maximum mass and volume budget allocated to the mission. The assessment phase as been used to consolidate a preliminary mass, volume and power break down between sub-systems.

Once in orbit, and because of the small instrument field of view (0.5 deg²) compared to the size of the survey (20 000 deg²), the observing strategy will be to step and stare the telescope keeping the Solar Aspect Angle between the Satellite Sun-shade and the Sun constant in order to minimize thermal variations. The inefficiencies of this strategy (slew and stabilization time between observed fields) must be kept to a level that ensures the 40 000 fields to be collected in less than 5 years, which is the mission duration.

Optimization of the survey strategy is required because of specific features inherent to the cosmological scales information probed by weak lensing. If specific spatial patterns are introduced in the survey image by regular gaps or inhomogeneities of the data, their impact in the Fourier space of the signal that is search could bring power in from scales where the theoretical uncertainties in the power spectrum are considerable (see figure 6).

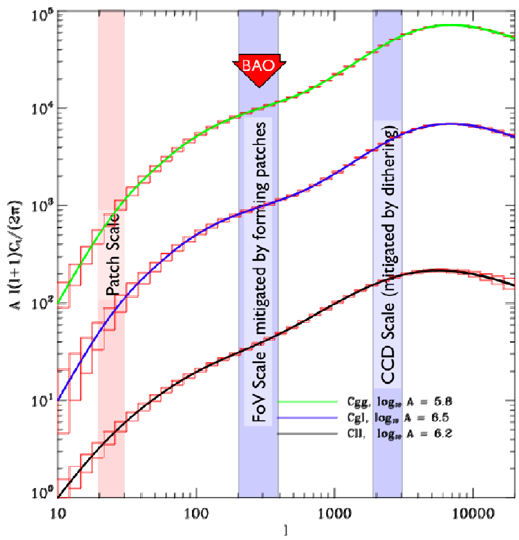

Figure 6. Illustration of the power spectra of the observable Euclid quantities as a function of scale l. This scale, l, is the inverse of angular scale θ [radians]. From top to bottom the three curves show (i) the galaxy-galaxy, (ii) the galaxy-lensing and (iii) the lensing-lensing power spectra along with the error bars that we would expect from Euclid. Also shown is the BAO scale. In blue bands we show the scales that correspond to the Euclid detectors and the FoV. We see that these scales lie in the range of interested that will be probed by Euclid. In red we show the scales that correspond to a patch (figure credit A. Amara & Julien Carron).

The effect of two typical instrument scales must be particularly mitigated. The field of view scale pattern effect (~0.5 deg²) is mitigated by constructing the survey in consecutive patches of 10x10 deg² area where homogeneity of the data is high. As the field of view of the instrument is large with a high sampling requirement, the Focal Plane Arrays covering the visible and NIR fields of view are composed of several detectors assembled together. The assembly of several arrays leads to mechanical gaps between the individual detectors with typical scale of 50 arcmin² and gaps of a 100 arcsec. Those gaps are mitigated by the constructing each observed instrument field of view out of 4 frames. Each frame is dithered from the previous one by a small step, the exact dithering pattern being optimized to minimize the remaining fraction of pixels not cumulating enough integration time to reach SNR on objects, and randomize the pattern of these pixels to suppress the pattern effect. The reference dithering strategy is obtained with 4 frames and 3 consecutive dither steps of ~100 arcsec, with a 2-dimension scanning approach allowing to ensure that more than 90% of the pixels in the visible and in the NIR can integrate over 3 (out of the 4) frames. The required SNR on reference object defined in section 2 must therefore be obtained after cumulating integration time on 3 frames (figure 7).

The dithering strategy also helps to mitigate the effect of clusters of bad pixels and cosmic rays, to improve the PSF calibration and galaxy shape measurement from sub-pixel information, to provide for a distortion map, and to allow for cross-correlations between exposures.

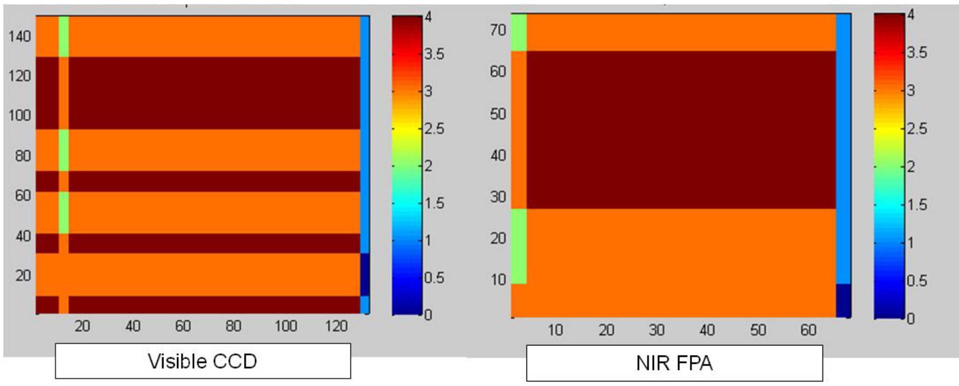

Figure 7. Number of frames (and hence integration time) seen by individual pixels of a visible and NIR detector. The pixel seing more than 3 frames cumulate sufficient integration time to reach required SNR on reference object.

Evaluation of the radiometric performance of the instrument allows building the reference observation strategy sequence based on a 4 frames sequence per instrument field of view, and construction of 20x20 deg² patched out of individual field of views. The visible and NIR imaging channels observe in parallel the same fields. The reference observation schemes, is based on visible frames of 450 s, in parallel, the 3 NIR wavebands are observed. Between each frame a dither is achieved at satellite level. At the end of the 4 frames, the satellite slews to the next field constructing the patch with strips of 1x20 deg².

This strategy allows for 36 fields per day, leading to a maximum of 500 Gbits generated in the visible and 200 Gbits in the NIR that fit within the allocated 850 Gbits maximum total amount of data per day.

3.2 Telescope Optical Architecture

The drivers for the telescope design are derived from the primary science requirement and from the boundary limits of the study, aiming at ensuring feasibility of the mission within programmatic constraints. The primary key parameters for the optical design are primary mirror size, instrument field of view, and instrument focal length in the different wavebands.

- Primary mirror diameter: the trade off is to have a primary large enough to ensure the observation of objects, and small enough to keep payload within size and mass allocation of the launcher capability (primary mirror is one of the parameters directly impacting the satellite size), and within manufacturing feasibility limits. The selected mirror diameter is 1.2m.
- Field of View: the trade off is to have the largest Field of View, as the mission is a survey mission. The larger the instrument field of view, the less satellite step-and-stare pointing are required to cover the sky area, each step introducing survey inefficiencies for satellite motion and stabilization limiting the effective observation time of the instruments. The field of view must be kept small as telescope as optical aberration increase rapidly with field size.
- Focal length: The focal length is derived from the pixel plate scale requirement and pixel physical scales actual feasibility. The reference pixels scales for the selected detectors are 12 µm for the visible and 18 µm in the IR leading to a 24 m focal length in the visible and 12 m focal length in the IR. The optical design shall optimize the telephoto parameter, defined as the ratio of the system effective focal length (EFL) to the length of the optical package to adapt the volume of the telescope to the satellite allocated envelop.

The reference telescope for the Assessment phase study is a design proposed by ESA. The optical concept is based on a Korsch-like F/20 three-mirror telescope. All three mirrors (M1, M2 and M3) are pure conic (no high order aspherical terms) and they are common to the VIS and NIP channels. In addition, the NIP channel has a set of 4 lenses (L1, L2, L3 and L4) that converts the F/20 beam into an F/10. VIS and NIP look at the same portion of sky simultaneously. The field of view is centered on an off-axis point. In consequence, the third mirror is used off-axis. This allows us to place the dichroic at the pupil image and separate VIS and NIP channels. The dichroic reflects the VIS beam and transmits the NIP beam.

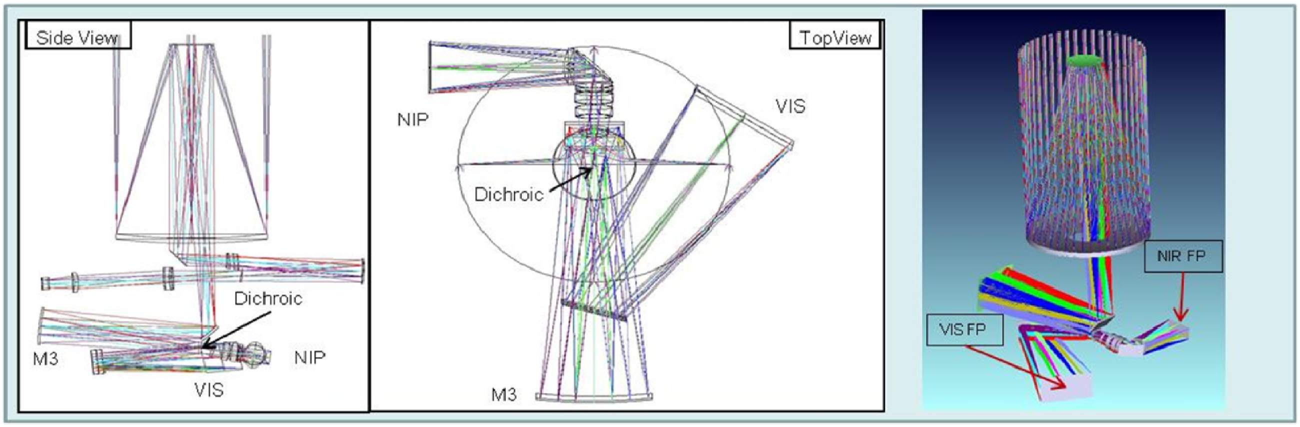

Figure 8. *Euclid* reference optical design and proposed packaging

Optical quality and stability driver is the visible channel requirement for very high image quality and stability. The design is optimized to be diffraction limited over the whole field of view on the visible waveband and to be wavelength independent (no lens on the visible path). A tolerancing analysis has been performed to estimate the sensitivity of the design showing that the most constraining parameters are the relative positions of M1 and M2 (X/Y position and tilt) and the very demanding surface error for all mirrors (10 to 15 nm RMS), which will require accurate polishing (figure 9).

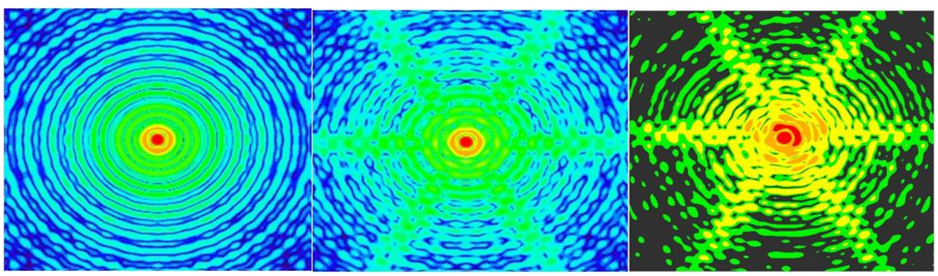

Figure 9. *Euclid* reference visible PSF for nominal optical design (left) nominal with 3 vanes M2 spider (centre) and tolerance with 3 vanes spider (right)

A statistical analysis (Monte-Carlo) is performed and shows that 98% of the trials have an average WFE (averaged over the field of view) better than 56nm RMS, and 90% of the trials have an average WFE better than 5nm RMS.

3.3 Instrument Architecture

The Euclid Imaging Instrument is composed of a Visible and a Near Infrared Imaging Channels providing shape measurements in the visible and photo-z information in the near infrared. It is optimized to fulfill the needs of the weak lensing science goals presented in section 2. During the assessment phase, the Euclid Imaging Channels optical interface is defined after the telescope M3 mirror. As the interface to the payload module (PLM) is not defined at that level, the working assumption in the current concept of the Euclid Imaging consortium is that VIS and NIP channels would be delivered integrated on a common composite support structure (COMA = Common Opto-Mechanical Assembly) ensuring mechanical and thermal interface. Three electronics boxes are associated to the instrument and integrated on the Payload, the Payload Data Handling Unit (PDHU) and the Payload Mechanism Control Unit (PMCU) and the NIP electronics CCU.

The COMA structural element is conceived as an aluminum honeycomb and carbon fiber sheets bench holding the two VIS and NIP channels, but also the dichroic and the fold mirror of the visible path, and supporting additional functions such as a shutter for visible read out and a visible calibration unit. The COMA would provide the thermal and mechanical interface towards the payload and ensure optical baffling to the VIS/NIP channels.

The fold mirror is a 290 mm x190 mm flat mirror with alignment capability through 3-balls joint for fine tuning of the focus on the VIS-FPA. The dichroic is a 120 mm in diameter plate that separate the visible wavelength range (reflection) and the NIR wavelength range (transmission). The calibration unit in the visible path consists of 3 visible LEDs at 600 nm, 750 nm and 900 nm with a lambertian diffuser in front of it and located below the VIS fold mirror. It allows illumination of the VIS Focal Plane Array with flatness better than 5% for calibration. The shutter mechanism is located in front of the dichroic it allows flat fielding of the visible channel and prevents trails formation in the images during readout.

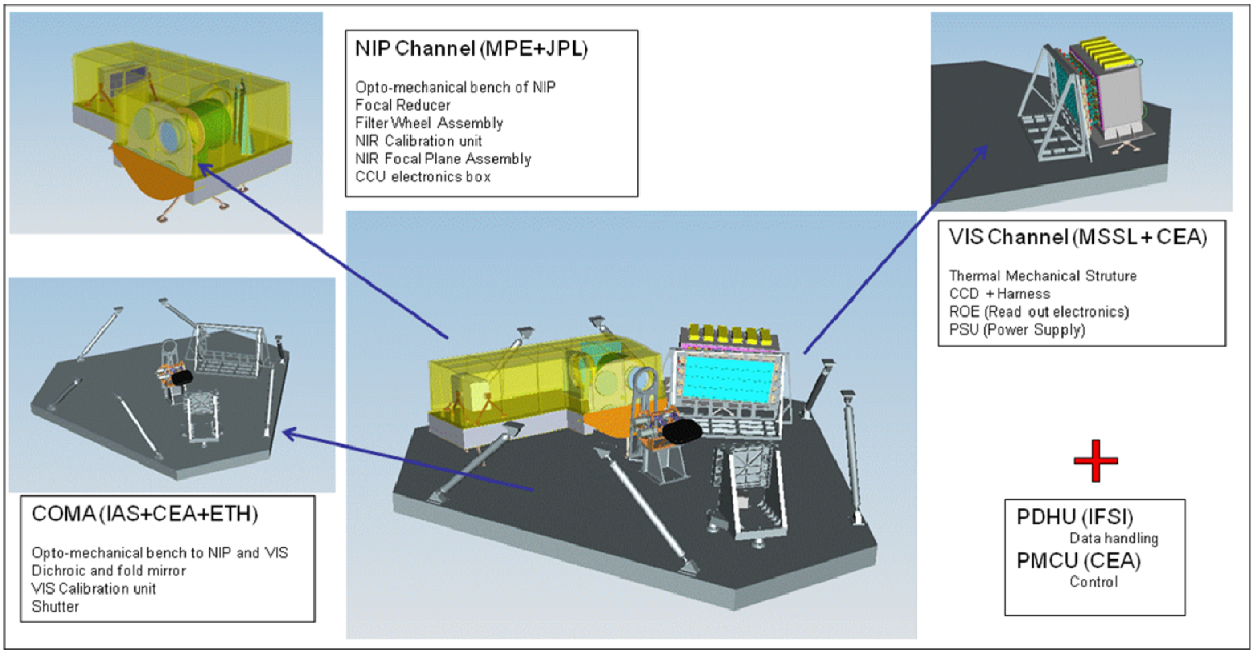

Figure 10. *Euclid* Imaging Channels instrument assembly and sub-systems

The thermal architecture assumes that the PLM structure is cooled down passively by the satellite to ~150K. The instrument is isolated from the radiative environment by MLI and dedicated radiators for the NIP structure (150 K) the NIR FPA (100 K), the VIS FPA (150 K) and the VIS electronics (240−300 K) are directly located on the cold side of the spacecraft. The NIP, the VIS FPA and the VIS electronics are thermally decoupled from the PLM bench for accurate thermal control.

The proposed electrical architecture is relying on 3 layers (see figure 11). The first layers is related to the detectors, both VIS and NIP and proximity electronics. The proximity electronics house all the functions required to control the temperature stability of detectors and process analog signals provided by them. The next layer is related to intermediate functions located close to the first layer either to keep electrical perturbation as low as requested (e.g. secondary power supply lines) or to limit harness length and hence capacitive load of low fan-out electronics (e.g. NIP front end). Interfaces between the first layer and the second one is either digital (digitized detector output signals) or for power distribution toward the detector electronics. Additionally this layer comprises the unit in charge of the control of the mechanical / thermal / calibration items for both VIS and NIP imagers. Finally the third and last layer is the payload centralized computer in charge of the instrument sub-system control and of the final data processing (lossless compression). This design has several benefits: it defines sub-systems that can be easily tested before delivery (VIS, NIP, mechanisms…). The centralized payload computer (PDHU) allows simplifying interfaces with the platform by merging all the control / command and data interfaces into one or two only. Flexibility is also increased with respect to system where detectors electronics are directly connected to the platform since the PDHU functions are implemented in software while detector electronics are mainly hardwired electronics.

The present electronic design is fully compliant with the performances of available technologies for serial interfaces, memory buffering and computing power: no critical issue is foreseen. Further studies will mainly focus on consolidation and optimization of sub-system internal design.

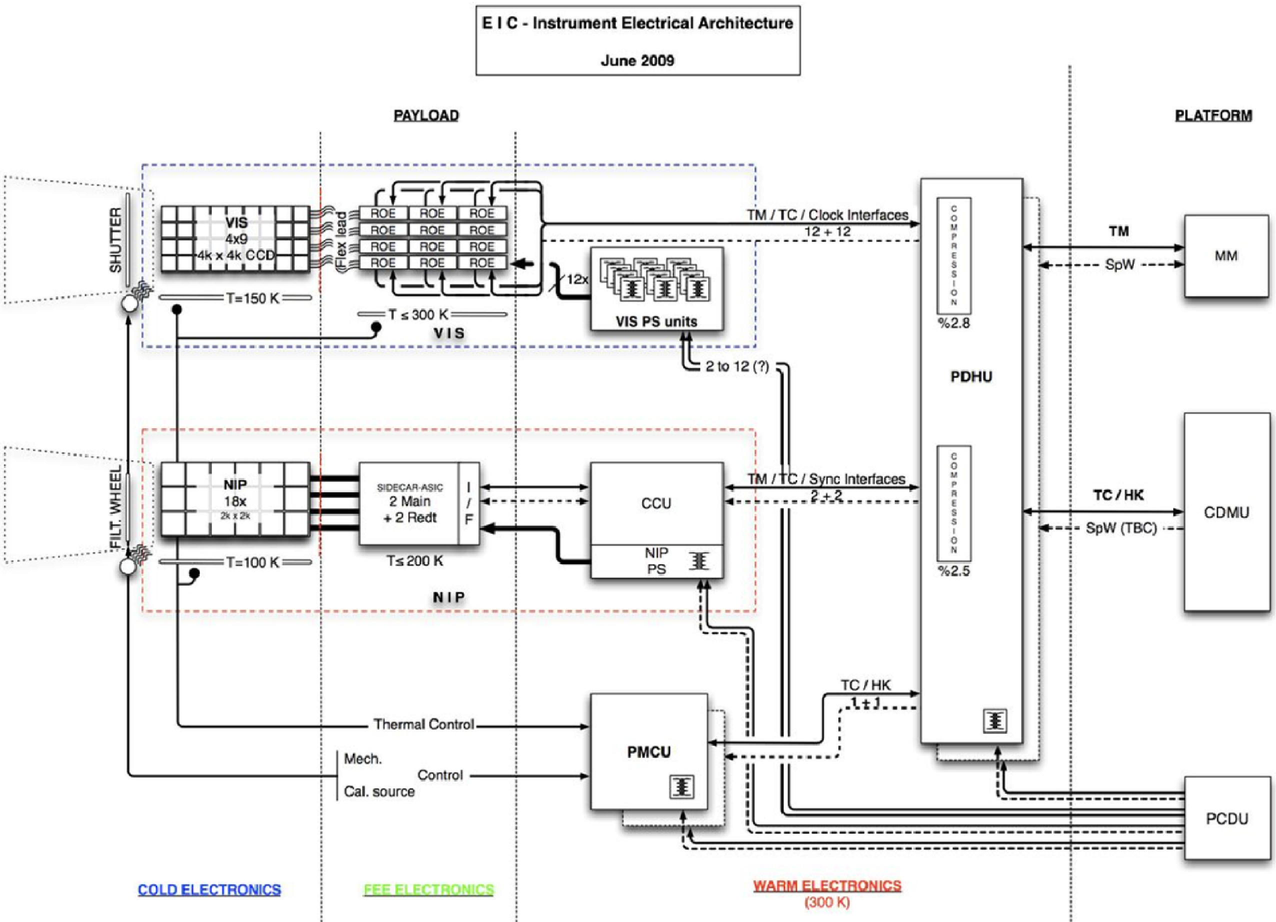

Figure 11. *Euclid* Imaging Channels electronics architecture

Full description of the VIS imaging channel and the NIR Photometric channel can be found in the following papers of the current SPIE conference: [10] Cropper, M. et al "VIS: the visible imager for Euclid". [9] Schweitzer, M. et al "NIP: the near-infrared imaging photometer for Euclid".

Additional information on the instrument design and performance can be found in the following posters of the current SPIE conference: Di Giorgio, A.M. et al, The data handling unit of the Euclid imaging channels: from the observational requirements to the unit architecture. Glauser, A et al, An optical shutter for the Euclid imager. Holmes, R. et al, The Euclid near-infrared calibration source. Holmes, R. et al, The filter wheel mechanism for the Euclid near-infrared imaging photometer.

4. LATEST DEVELOPMENTS

The current status of *Euclid*, as it moves towards its definition phase, is presenting some notable differences with the reference design of the assessment phase. The main change comes from the merging of the NIR photometric channel and the NIR spectroscopic instrument into a single instrument performing both functions.

The optical design is being refined to accommodate this change and the satellite architecture will be adapted. The science parameters remain the same but the mission is heading toward a new configuration that is currently being defined.

REFERENCES

[1] Réfrégier et al, "Euclid Imaging Consortium Science Book," arXiv:1001.0061v1, (2010).

[2] Laureijs, R. et al, “The Euclid Mission,” SPIE 7731, (2010)

[3] Amara, A., Réfrégier, A., “Optimal surveys for weak-lensing tomography,” MNRAS 381,1018-1026, (2007)

[4] Bridle, S., King, L., “Dark energy constraints from cosmic shear power spectra: impact of intrinsic alignments on photometric redshift requirements,” New Journal of Physics, 9, 444, (2007)

[5] Abdalla, F. B., Amara, A., Capak, P., Cypriano, E. S., Lahav, O., & Rhodes, J., “Photometric redshifts for weak lensing tomography from space: the role of optical and near infrared photometry,” MNRAS, 387 , 969-986, (2008)

[6] Bordoloi, R., Lilly, S. J., & Amara, A., “Photo-z Performance for Precision Cosmology,” ArXiv e-prints, (2009)

[7] Meneghetti, M., Melchior, P., Grazian, A., De Lucia, G., Dolag, K., Bartelmann, M., Heymans, C., Moscardini, L., Radovich, M., “Realistic simulations of gravitational lensing by galaxy clusters: extracting arc parameters from mock DUNE images,” A&A, 482 , 403-418, (2008)

[8] Massey, R., Refregier, A., Conselice, C. J., David, J., & Bacon, J., “Image simulation with shapelets,” MNRAS, 348 , 214-226, (2004)

[9] Schweitzer, M. et al, “NIP: the near-infrared imaging photometer for Euclid,” SPIE 7731, (2010)

[10] Cropper, M. et al, “VIS: the visible imager for Euclid,” SPIE 7731, (2010)